Electrocatalysis of the Heat-Treated (5,10,15,20-Tetraphenylporphyrinato)-manganese(III) Halides for Cathodic Reduction of Oxygen

Osamu IKEDA,* Toyosei KOJIMA, and Hideo TAMURA
Department of Applied Chemistry, Faculty of Engineering, Osaka University, Yamadaoka, Suita, Osaka 565
(Received December 20, 1985)

Electrocatalysis of the heat-treated (5,10,15,20-tetraphenylporphyrinato)manganese(III) halides (Mn^{III}(TPP)X, X:F^-, Cl^-, Br^-, I^-) for the O_2 reduction in an alkaline solution has been studied by rotating ring-disc electrode technique, and the result was correlated with properties of the heat-treated Mn^{III}(TPP)X, such as magnetic moment and electrical resistivity. The axial ligand X showed noticeable effect on the catalytic activity. The catalytic activity estimated from the overpotential changed in the following order: $F^->Cl^->Br^->I^-$. The catalytic activity for reducing oxygen to OH^- was low, but the same order of activity as the above applies. The order was interpreted by the σ-donating ability of halide ion X to d_{z^2} orbital. The active site of the Mn^{III}(TPP)X heat-treated at 700 °C for O_2 reduction is ascribed to the metal ion, coordinated to slightly degraded or perfect N_4 center, but not degradation products of the relevant compounds.

Many transition metal complexes with macrocycles such as porphyrin, phthalocyanine, and tetraaza-annulene show catalytic activity for the cathodic reduction of oxygen. When these metallomacrocycles are applied to practical electrocatalyst for O_2 reduction, however, many of them are unstable in strong acid and alkaline electrolytes. Jahnke et al.[1] showed that this defect is overcome by the heat treatment in an inert atmosphere, and that the catalytic activity improved by the treatment. The disclosure accelerated the study on the heat treatment of metallomacrocycles for the cathodic reduction of oxygen.[2-15] However, the active site and the electrocatalysis of the heat-treated metallomacrocycles have not been fully elucidated. The active site suggested so far is (i) metal ion in the N_4 center,[7,16] (ii) carbonaceous substance formed by the degradation of N_4 center,[4] and (iii) an intermediate between (i) and (ii), namely, metal ion coordinated to partially degraded N_4 center.[13] The finely dispersed metal such as β-cobalt, which is formed by the heat treatment of cobalt(II) porphyrins, is examined.[11]

Recently, we studied the cathodic reduction of oxygen on unheated Mn^{III}(TPP)X, whose various properties are influenced by the axial ligand because of the strong π-mixing between metal and porphyrin ring.[17-20] It follows that the catalytic activity for O_2 reduction strongly depends on the axial ligand.[21] The porphyrins seem to be suitable to investigate active site and the electrocatalysis of heat-treated metallo-porphyrins for O_2 reduction, because the axial ligand affects the electrocatalysis, if the metal ion is the active site.

Experimental

Materials. In analogy with octaethylporphyrinatoiron-(III) halides,[22] Mn^{III}(TPP)X (X:F^-, Cl^-, Br^-, I^-) were prepared by the ligand-exchange reaction of Mn^{III}(TPP)($OCOCH_3$) with aqueous NaX as described elsewhere.[21] Plates (10×10 mm^2) and rods (6 mmϕ) of glassy carbon (G.C., Tokai Carbon, GC20) were used as the base electrode, onto which one of the Mn^{III}(TPP)X was coated. These G.C. electrodes were polished to a mirror surface with alumina powder, and washed in an ultrasonic bath to remove alumina powder. 1 M(=mol dm^{-3}) KOH was used as the electrolyte, which was saturated with pure oxygen at the cathodic reduction experiments. Pt net and Hg/HgO electrode in 1 M KOH were used as counter and reference electrodes, the potential of the latter against normal hydrogen electrode (NHE) being +0.098 V.

Heat Treatment. The chloroform solution of each Mn^{III}(TPP)X was coated onto the G.C. plate (1 cm^2) and top surface of the rod (0.28 cm^2) using a microcyringe, and the coating amount was fixed to 3×10^{-7} mol cm^{-2}. After drying in air, the electrodes were placed in a quarz tube, and then filled with highly pure Ar (O_2<1—2 ppm) by alternate degassing and filling. The Mn^{III}(TPP)X-coated G.C. in the tube was heated in an electric furnace for 10 min at each temperature and cooled in air. Electrochemical data for heat-treated Mn^{III}(TPP)X varied with the amount of coating, probably due to imperfect coating and sublimation up to less than 1×10^{-7} mol cm^{-2}. However, the data became nearly constant at the coating over 1×10^{-7} mol cm^{-2}.

The heat treatment of Mn^{III}(TPP)X powder, for the measurement of bulk properties, was carried out by the same manner as described above by putting the powder in a small quarz beaker.

Electrochemical Measurements. The G.C. rod coated with heat-treated Mn^{III}(TPP)X was used as the ring (Pt)-disc electrode. The Pt ring was cleaned by a potential sweep cycling between O_2 and H_2 generation potentials in 0.5 M H_2SO_4 before use. In the cathodic reduction of oxygen, the ring potential was fixed to +0.25 V (vs. Hg/HgO in 1 M KOH), where the diffusion limiting current for HO_2^- oxidation was observed.

The G.C. plate coated with heat-treated Mn^{III}(TPP)X was installed into a Teflon holder with a window of 0.5 cm^2 open to the electrolyte solution, and was used in the cyclic voltammetry to evaluate catalytic activity and stability.

Other Measurements. The mass magnetic susceptibility

* Present address: Laboratory of Chemistry, College of Liberal Arts, Kanazawa University, 1-1 Marunouchi, Kanazawa 920.

χ_g of heat-treated Mn^{III}(TPP)X was measured by Gouy method using a magnetic balance (Shimadzu, MB-11) at room temperature, usually 25 °C. The χ_g was corrected for ferromagnetic impurities by extrapolating the plot of (mass magnetization)/(magnetic field strength) [$(M)/(H)$] against $(1/H)$ to $(1/H)=0$. The molar magnetic susceptibility χ_M was evaluated by determining the molecular weight (M.W.) of the porphyrin unit per manganese ion, using the relation: $\chi_M=\chi_g \times$M.W. Thermogravimetry (TG) and differential thermal analysis (DTA) for Mn^{III}(TPP)X were carried out by means of Rigaku DG-ClH Thermoflex, at a heating rate of 5 °C min^{-1} in Ar stream. Electrical resistivity of heat-treated Mn^{III}(TPP)X was measured by the two-probe method for powdered sample pressed between metal rods in a thick glass tube.

Results and Discussion

Thermal Behavior of Mn^{III}(TPP)X. Thermal reactions taking place during the heat treatment were elucidated from the DTA and TG curves. The results for four Mn^{III}(TPP)X (X:F^-, Cl^-, Br^-, I^-) examined are shown in Fig. 1. The DTA curve of each porphyrin has two endo/exothermic peaks at nearly same temperature regions: The first is between 400° and 500 °C, and the second around 850 °C. An obvious weight loss was observed in TG curves at the first DTA peak, but not at the second DTA peak. The first thermal reaction between 400° and 500 °C is speculated to be the condensation reaction due to release of phenyl groups and hydrogen, indicating formation of an extended π-electron system, because the resistivites of Mn^{III}(TPP)X decreased from $>10^9\ \Omega$ cm to 10^5—$10^4\ \Omega$ cm with this reaction. The second thermal reaction seems to be the degradation of porphyrin skeleton, because manganese monoxide (MnO) was detected by X-ray diffraction in the samples heated above 850 °C.

The following analyses examine the changes in the heat treatment of Mn^{III}(TPP)X. Some properties of Mn^{III}(TPP)X heat-treated at 700 °C were compared, where the catalytic activity for O_2 reduction is maximum.

Molecular Weight. Since Mn^{III}(TPP)X heat-treated above 500 °C are insoluble in organic solvents, the molecular weight per manganese ion was evaluated by determining Mn ion in the ashed samples on heating in air. Table 1 summarizes the results. The accuracy of this measurement is ±3% from the results for unheated Mn^{III}(TPP)X. The molecular weight decreased with the heat treatment at 700 °C by 60—90. This suggests a release of one phenyl group during the heat treatment. Release of hydrogen atoms on phenyl groups may occur at 700 °C, because the condensation products show no solubility in organic solvents and have low resistivity of about $10^2\ \Omega$ cm.

Atomic Ratio. In order to examine the stability of N_4 center during the heat treatment, the atomic ratio of N to Mn was evaluated using the manganese content and the nitrogen content obtained from the elemental analysis. Figure 2 shows the results as a function of the heat-treatment temperature. The N/Mn ratio for unheated Mn^{III}(TPP)X was about 4,

Table 1. Molecular Weight Per Manganese Ion for Unheated and Heat-Treated Mn^{III}(TPP)X

X	Heat-treatment temperature/°C			
	unheated	500	700	900
F^-	670	630	600	580
Cl^-	720	—	630	—
Br^-	760	—	700	—
I^-	800	—	740	—

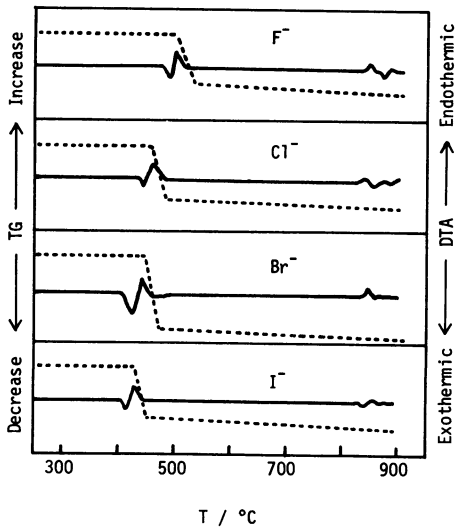

Fig. 1. Differential thermal analysis (——) and thermogravimetry (----) curves for Mn^{III}(TPP)X (X: F^-, Cl^-, Br^-, I^-) in Ar stream. Heating rate, 5 °C min^{-1}.

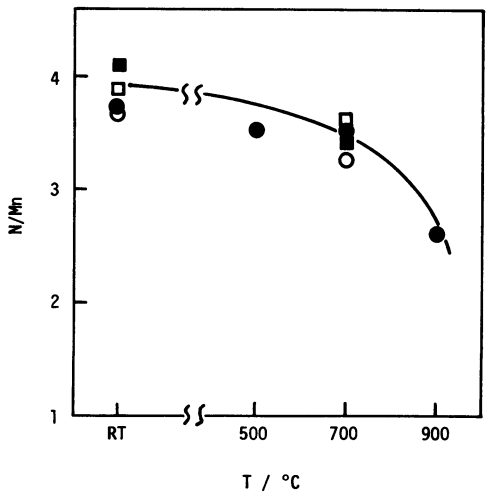

Fig. 2. Variation of N/Mn ratio with the heat-treatment temperature for Mn^{III}(TPP)X. X: (●) F^-; (■) Cl^-; (□) Br^-; (○) I^-. RT(room tempereature) means the unheated Mn^{III}(TPP)X.

while the ratio gradually decreased to 3.5 with the heat treatment up to 700 °C, and greatly fell to 2.6 at 900 °C. The results suggest that the N_4 center is maintained up to 700 °C, but it is degraded at 900 °C where the second DTA peak appears and MnO is detected by X-ray diffraction.

Next, we determined the ratio of X to Mn to estimate the stability of Mn–X bond in the heat treatment, using the molecular weight per manganese ion and the X content from the elemental analysis. The X/Mn ratio for Mn^{III}(TPP)X heat-treated at 700 °C, except for Mn^{III}(TPP)F whose elemental analysis for F was impossible, was 0.8—0.9. This suggests that most of the manganese sites are coordinated by the axial ligand even after the heat treatment at 700 °C.

Magnetic Moment. Magnetic moment for Mn^{III}(TPP)X heat-treated at 700 °C was evaluated to estimate the spin state of central manganese ion. The effective magnetic moment μ_{eff} was calculated by the following relation for magnetically diluted substances: $\mu_{eff}=2.84\sqrt{\chi_M T}$, where T is the temperature at the measurement. The μ_{eff} for all Mn^{III}(TPP)X (X: F^-, Cl^-, Br^-, and I^-) heat-treated at 700 ° were in the range of 5.0—5.3 μ_B (Bohr Magneton) and were in good agreement with the values of 5.0—4.8 μ_B for unheated Mn^{III}(TPP)X (X: Cl^-, Br^-, and I^-), a fact indicating high-spin $Mn^{III}(d^4)$ complex which has the theoretical μ_{eff} of 4.9 μ_B. The μ_{eff} of unheated Mn^{III}(TPP)F was 3.8 μ_B. The result indicates that an intermediate-spin changed to the high-spin complex by the heat treatment, as can be seen from Fig. 3. We confirmed previously that the unheated Mn^{III}(TPP)F has the highest π-mixing with ring orbitals among Mn^{III}(TPP)X.[21] Extended π-electron system due to the heat treatment seems to weaken the π-mixing, resulting in high-spin state.

Electrocatalysis for O_2 Reduction. We have discussed the electrocatalysis of heat-treated Mn^{III}(TPP)X based on two methods to examine the catalytic activity: One is the overpotential and the other the capability of reducing oxygen to OH^- or the so-called 4-electron reducibility.

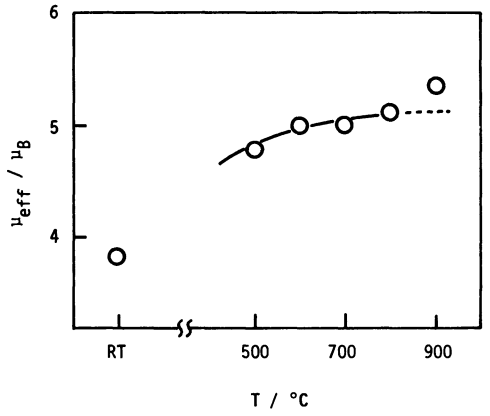

Fig. 3. Variation of the effective magnetic moment (μ_{eff}) of Mn^{III}(TPP)F with heat-treatment temperature. RT(room temperature) means the unheated Mn^{III}(TPP)F.

Figure 4 shows the voltammograms of Mn^{III}(TPP)F heat-treated at different temperatures for the O_2 reduction by rotating disc electrode. The catalytic activity based on the overpotential or the current at a constant potential showed a complicated change with the heat-treatment temperature: It decreased with the temperature up to 600 °C, and then increased showing a maximum at 700 °C. The same change was also observed in the cyclic voltammograms by use of plate electrode. The catalytic activity fluctuated at 800 °C: Low reproducility at 800 ° seems to be related with that the temperature is in the vicinity of the degradation temperature of N_4 center. The low catalytic activity of Mn^{III}(TPP)F heat-treated at 900 °C is caused by the degradation of N_4 center. The diffusion limiting current for O_2 reduction became lower by the heat treatment, indicating the change in reduction pathway from the 4-electron pathway ($O_2+2H_2O+4e^-\rightarrow 4OH^-$) to the 2-electron pathway ($O_2+H_2O+2e^-\rightarrow HO_2^-+OH^-$), as will be discussed later.

Figure 5 shows the cyclic voltammograms of Mn^{III}(TPP)X heat-treated at 700 °C. Under more negative potentials, the reduction peak in the cyclic voltammogram was observed for Mn^{III}(TPP)Br, but unobservable for Mn^{III}(TPP)I. However, the catalytic

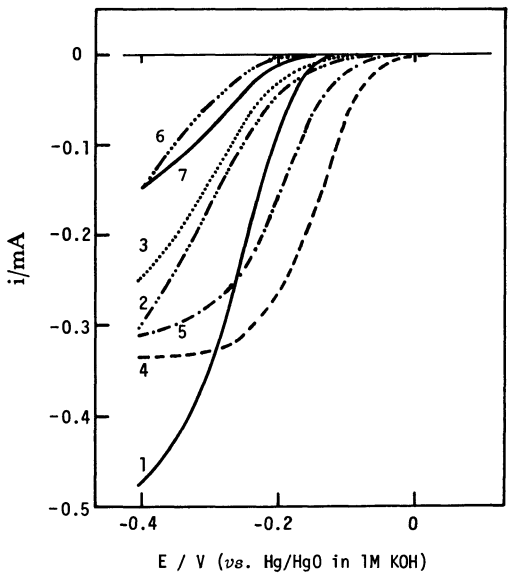

Fig. 4. Voltammograms at the rotating disc(glassy carbon coated with Mn^{III}(TPP)F) electrode for the cathodic reduction of oxygen in O_2-saturated 1M KOH. Heat-treatment temperature of Mn^{III}(TPP)-F: (1) unheated; (2) 500 °C; (3) 600 °C; (4) 700 °C; (5) 800 °C; (6) 900 °C; (7) bare G.C. Sweep rate, 20 mV s^{-1}; rotation rate, 1000 r.p.m.; surface area of the disc, 0.28 cm^2.

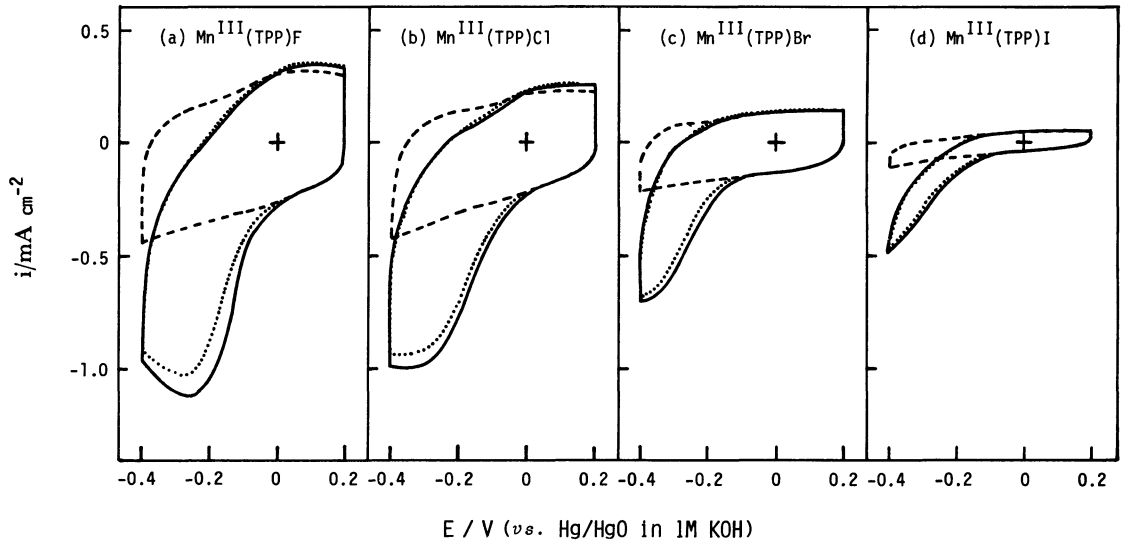

Fig. 5. Cyclic voltammograms at the plate(glassy carbon coated with Mn^{III}(TPP)X heat-treated at 700 °C) electrode for the cathodic reduction of oxygen in O_2-saturated 1 M KOH. X: (a) F^-; (b) Cl^-; (c) Br^-; (d) I^-. The broken line is for N_2-saturated 1 M KOH. The solid and dotted lines for O_2-saturated 1 M KOH are the voltammograms at the first cycle and after 1000 cycles, respectively. Sweep rate, 100 mV s^{-1}; electrode area, 0.5 cm^2.

activity estimated from the overpotential was in the order: $F^->Cl^->Br^->I^-$. Stability of the catalysts was improved by the heat treatment, because there appeared only a small change in the cyclic voltammograms at the first and 1000 cycles (Fig. 5). Since the instability of unheated Mn^{III}(TPP)X depends upon the ligand exchange of X with OH^-,[21] the improved stability suggests the formation of a dense structure without pores which prevents from penetrating of electrolyte.

Figure 6 shows the voltammograms at the rotating ring (Pt)-disc (G.C. coated with Mn^{III}(TPP)X heat-treated at 700 °C) electrode. The lower curves represent the disc currents for O_2 reduction and the upper curves the ring currents for the oxidation of HO_2^- as a reduction intermediate of O_2.

In order to elucidate the 4-electron reducibility of the heat-treated Mn^{III}(TPP)X for oxygen, the apparent number of electrons consumed in the O_2 reduction (n_{app}) was evaluated using the ring and disc currents around −0.3 V in Fig. 6. In the evaluation of n_{app}, it was assumed that the O_2 reduction at the disc consists of a mixed reaction of the 2-electron pathway ($O_2+H_2O+2e^-\rightarrow HO_2^-+OH^-$) and the 4-electron pathway ($O_2+2H_2O+4e^-\rightarrow 4OH^-$). Thus n_{app} was estimated by the next relation:[15,23] $n_{app}=4I_{Disc}/(I_{Disc}+I_{Ring}/N_{corr})$, where N_{corr} is the collection efficiency for HO_2^-, corrected for a deviation from the coplanality between the Pt ring and the Mn^{III}(TPP)X-coated disc, which is about 0.1 for various ring-disc electrodes.

The result for Mn^{III}(TPP)X heat-treated at 700 °C is shown in Fig. 7. Also, the result for Mn^{III}(TPP)F heat-treated at different temperatures is shown in Fig. 8. As can be seen from Fig. 7, the n_{app} shows some

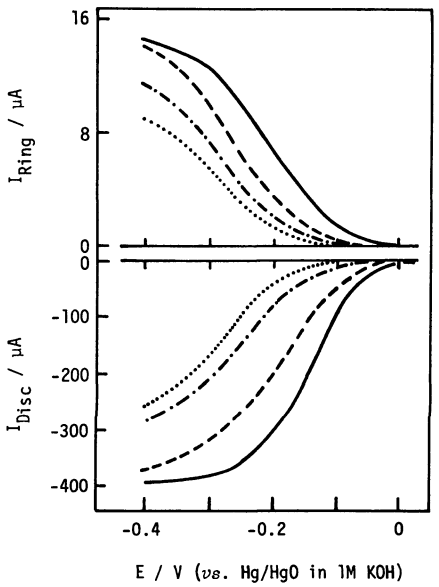

Fig. 6. Voltammograms at the rotating ring(Pt)-disc (glassy carbon coated with Mn^{III}(TPP)X heat-treated at 700 °C) electrode for the cathodic reduction of oxygen in O_2-saturated 1 M KOH. X: (——) F^-; (----) Cl^-; (—·—) Br^-; (·····) I^-. Ring potential, 0.25 V (vs. Hg/HgO in 1 M KOH); sweep rate at the disc, 20 mV s^{-1}; rotation rate, 1000 r.p.m.; surface area of the disc, 0.28 cm^2.

dependence on the axial ligand, and the n_{app} value decreases from 2.3 for F^- to 2.0 for I^-. On the other hand, it is observed from Fig. 8 that the high 4-electron reducibility of unheated Mn^{III}(TPP)F is considerably lost by the heat treatment.

Effect of Axial Ligand on Electrocatalysis. The catalytic activity of heat-treated Mn^{III}(TPP)X, based

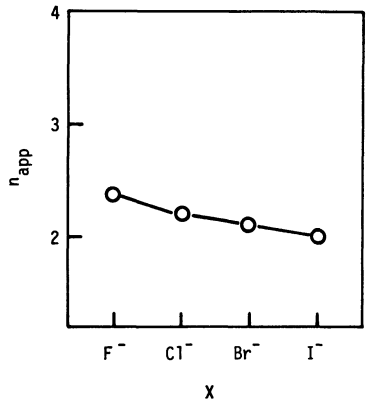

Fig. 7. Variation of the apparent number of electrons consumed in O_2 reduction (n_{app}) with the axial ligand of $Mn^{III}(TPP)X$ heat-treated at 700 °C.

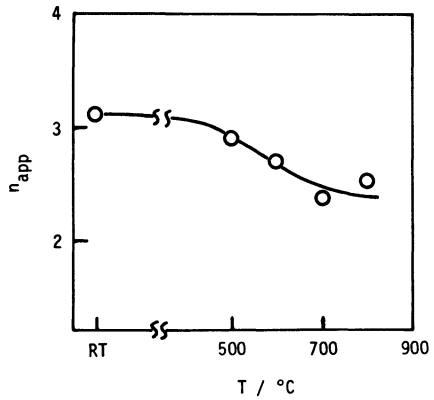

Fig. 8. Variation of the apparent number of electrons consumed in O_2 reduction (n_{app}) with the heat-treatment temperature for $Mn^{III}(TPP)F$. RT(room temperature) is for the unheated $Mn^{III}(TPP)F$.

on the overpotential and the 4-electron reducibility, depends markedly on the axial ligand. As for the property of the axial ligand affecting the catalytic activity, the most probable one seems to be the electron-donating ability of X, which influences on interaction with O_2 molecule on manganese site through a change in the d-electron population.

The coordination mode of oxygen to metal has been considered to be an important factor for the catalysis or the reaction pathway in the cathodic reduction of oxygen. The end-on coordination (Pauling model[24]) leads to the 2-electron pathway, while the side-on coordination (Griffith model[25]) leads to the 4-electron pathway. Therefore, the d-electron configuration leading to the 4-electron pathway is considered to be empty d_{z^2} orbital which accepts electrons of oxygen $1\pi_u$ to form σ-bond, and filled d_{xz} and d_{yz} (d_π) orbitals which enable the back donation to oxygen $1\pi_g^*$ orbital.[26]

Figure 9 represents (a) the low-spin and (b) the high-spin d-electron configuration for a manganese-(III) porphyrin, respectively.[27] Though the high-spin

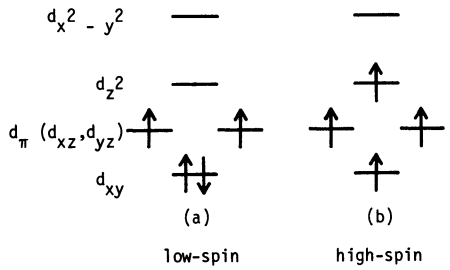

Fig. 9. The d-electron configurations for (a) low-spin and (b) high-spin d^4 manganese(III) porphyrin.

$Mn^{III}(TPP)X$ has half-filled d_π orbitals, the O_2 reduction on it occurs virtually through the 2-electron pathway. The presence of unpaired electron on d_{z^2} orbital seems to form predominantly the end-on coordination of oxygen through an interaction with $1\pi_g^*$ orbital, leading to the 2-electron pathway. The high 4-electron reducibility of unheated $Mn^{III}(TPP)F$ is ascribed to the intermediate spin, i.e., periodical or partial formation of the low-spin state with high affinity with the side-on coordination of oxygen. The 4-electron reducibility lowered by the heat treatment can be accounted for by the alteration into the high-spin state (Figs. 3 and 8). Irrespective of the high-spin state, the σ-donation by axial ligand onto d_{z^2} orbital seems to favor slightly the 4-electron reducibility because the character of unpaired electron of the d_{z^2} orbital is diluted by the donated electrons. In this context, the order of the electron-donating ability of X[17] ($F^- > Cl^- > Br^- > I^-$) explains the change in the 4-electron reducibility of heat-treated $Mn^{III}(TPP)X$ with X (Fig. 7).

The electron-donating ability of X thus explains the catalytic activity based on the overpotential (Fig. 5), because the increased population of electron on d_{z^2} orbital facilitates the interaction with O_2 molecule, as in the case of [tetrakis(methoxyphenyl)porphyrinato]-cobalt(II) with electron-donating methoxy groups.[28]

A particular phenomenon observed for heat-treated $Mn^{III}(TPP)X$ was the occurrence of large background current in Fig. 5. Moreover, the magnitude of the background current appears to represent the catalytic activity. This current is considered to be a capacitive current, as has already been confirmed for thick cobalt-phthalocyanine film,[29] which presumably has a characteristic surface state. As the surface state in the heat-treated $Mn^{III}(TPP)X$, delocalized π-electron in the extended π-system or metal may be conceivable. It has been noted for hydrophobic iron-porphyrin[23] that only the outermost layer of multiple layer on the electrode is effective on the electrocatalysis. Accordingly, the surface state described above will assist the electron transfer to oxygen molecule coordinated on the metal.

References

1) H. Jahnke, M. Schönborn, and G. Zimmerman, *Fortschr. Chem. Forsch.*, **61**, 133 (1976).
2) V. S. Bagozky, M. M. Tarasevich, K. A. Radyushkina, O. A. Levina, and S. I. Andrusyova, *J. Power Sources*, **2**, 233 (1977/78).
3) K. Wiesener and A. Fuhrman, *Z. Phys. Chem. (Leipzig)*, **261**, 411 (1980).
4) A. Fuhrman, K. Wiesener, I. Iliev, S. Gamburzev, and A. Kaisheva, *J. Power Sources*, **6**, 69 (1981).
5) J. A. R. van Veen, J. F. van Baar, C. J. Kroese, J. G. F. Coolegem, N. de Wit, and H. A. Colijn, *Ber. Bunsenges. Phys. Chem.*, **85**, 693 (1981).
6) J. A. R. van Veen and H. A. Colijn, *Ber. Bunsenges. Phys. Chem.*, **85**, 700 (1981).
7) J. A. R. van Veen, J. F. van Baar, and K. J. Kroese, *J. Chem. Soc., Faraday Trans. 1*, **77**, 2827 (1981).
8) A. Kaisheva, S. Gamburtsev, and I. Iliev, *Elektrokhimiya*, **18**, 139 (1982).
9) S. Gamburtsev, I. Iliev, and A. Kaisheva, *Elektrokhimiya*, **18**, 1602 (1982).
10) K. Okabayashi, O. Ikeda, and H. Tamura, *Chem. Lett.*, **1982**, 1659.
11) K. Wiesener, *Elektrokhimiya*, **18**, 758 (1982).
12) I. Iliev, S. Gamburtsev, A. Kaisheva, A. Fuhrman, and K. Wiesener, *J. Power Sources*, **13**, 217 (1984).
13) E. Yeager, *Electrochim. Acta.*, **29**, 1527 (1984).
14) O. Ikeda, H. Fukuda, and H. Tamura, *J. Chem. Soc., Chem. Commun.*, **1984**, 567.
15) O. Ikeda, H. Fukuda, and H. Tamura, *J. Chem. Soc., Faraday Trans. 1*, **82**, 1561 (1986).
16) R. W. Joyner, J. A. R. van Veen, and W. M. H. Sachtler, *J. Chem. Soc., Faraday Trans. 1*, **78**, 1021 (1982).
17) G. N. La Mar and F. A. Walker, *J. Am. Chem. Soc.*, **97**, 5103 (1975).
18) R. R. Gaughan, D. F. Shriver, and L. J. Boucher, *Proc. Nat. Acad. Sci. U.S.A*, **72**, 433 (1975).
19) L. J. Boucher, *Ann. N. Y. Acad. Sci.*, **205**, 409 (1973).
20) L. J. Boucher, *J. Am. Chem. Soc.*, **92**, 2725 (1970).
21) O. Ikeda, T. Kojima, and H. Tamura, *J. Electroanal. Chem. Interfacial Electrochem.*, **200**, 323 (1986).
22) H. Ogoshi, E. Watanabe, Z. Yoshida, J. Kincaid, and K. Kawamoto, *J. Am. Chem. Soc.*, **95**, 2845 (1973).
23) K. Shigehara and F. C. Anson, *J. Phys. Chem.*, **86**, 2776 (1982).
24) L. Pauling, *Nature*, **203**, 182 (1964).
25) J. S. Griffith, *Proc. R. Soc. London, Ser. A*, **235**, 23 (1956).
26) J. S. Valentine, *Chem. Rev.*, **73**, 235 (1973).
27) A. P. Hansen and H. M. Goff, *Inorg. Chem.*, **23**, 4519 (1984).
28) H. Alt, H. Binder, W. Lindner, and G. Sandstede, *J. Electroanal. Chem. Interfacial Electrochem.*, **31**, App. 19 (1961).
29) F. van den Brink, W. Visscher, and E. Barendrecht, *J. Electroanal. Chem. Interfacial Electrochem.*, **157**, 283 (1983).